Journal of Magnetic Resonance 348 (2023) 107391

Contents lists available at ScienceDirect

Journal of Magnetic Resonance

journal homepage: www.elsevier.com/locate/jmr

In-house fabrication of 1.3 to 7 mm MAS drive caps using desktop 3D printers

Cyriaque Amerein [a,1], Utsab Banerjee [a,1], Zhenfeng Pang [a], Wenqing Lu [b], Vanessa Pimenta [b], Kong Ooi Tan [a,*]

[a] Laboratoire des Biomolécules, LBM, Département de Chimie, École Normale Supérieure, PSL University, Sorbonne Université, CNRS, 75005 Paris, France
[b] Institut des Matériaux Poreux de Paris, Ecole Normale Supérieure, ESPCI Paris, CNRS, PSL University, 75005 Paris, France

ARTICLE INFO

Article history:
Received 22 January 2023
Revised 31 January 2023
Accepted 1 February 2023
Available online 6 February 2023

Keywords:
Magic-Angle Spinning
Solid-State NMR
3D Printing
Additive Manufacturing

ABSTRACT

The 3D-printing technology has emerged as a well-developed method to produce parts with considerably low cost and yet with high precision (<100 μm). Recent literature has shown that the 3D-printing technology can be exploited to fabricate a magic-angle spinning (MAS) system in solid-state nuclear magnetic resonance (NMR) spectroscopy. In particular, it was demonstrated that advanced industry-grade 3D printers could fabricate 3.2 mm MAS drive caps with intricate features, and the caps were shown to spin > 20 kHz. Here, we show that not only lab-affordable benchtop 3D printers can produce 3.2 mm drive caps with a similar quality as the commercialized version, but also smaller 2.5 mm and 1.3 mm MAS drive caps—despite a slight compromise in performance. All in-house fabricated drive caps (1.3 to 7 mm) can be consistently reproduced (>90 %) and achieve excellent spinning performances. In summary, the > 3.2 mm systems have similar performances as the commercial systems, while the 2.5- and 1.3-mm caps can spin up to 26 kHz ± 2 Hz, and 46 kHz ± 1 Hz, respectively. The low-cost and fast in-house fabrication of MAS drive caps allows easy prototyping of new MAS drive cap models and, possibly, new NMR applications. For instance, we have fabricated a 4 mm drive cap with a center hole that could allow better light penetration or sample insertion during MAS. Besides, an added groove design on the drive cap allows an airtight seal suitable for probing air- or moisture-sensitive materials. Moreover, the 3D-printed cap was shown to be robust for low-temperature MAS experiments at ~ 100 K, making it suitable for DNP experiments.

1. Introduction

Solid-state NMR is a powerful characterization technique that has been widely applied to study solid-state samples ranging from small molecules, biological macromolecules, to inorganic materials [1]. Although solid-state samples usually have broad peaks due to anisotropic interactions such as dipolar couplings and chemical-shift anisotropy, they can be averaged out by performing magic-angle spinning (MAS) experiments [2,3], where the sample is spun at an angle of 54.74° with respect to the static magnetic field. It is essential that the MAS frequency (ν_r) should be sufficiently larger than the size of the anisotropic interactions to achieve an efficient line-narrowing effect, i.e., the rotors can spin up to ν_r = 160 kHz depending on their sizes (Table 1) [4,5]. To achieve such fast MAS frequencies without significantly heating the NMR sample, the rotors are pneumatically spun with gas to reduce frictional heating. Besides achieving faster MAS frequencies, maintaining a stable spinning frequency (usually within a deviation of few Hz) is important over the course of experiments, especially for 2D or 3D NMR experiments that could last several days or week(s). Hence, the choices of material for both the rotor and MAS drive cap are important as they must be mechanically rigid (high tensile or flexural strength), and easily fabricated—especially the drive cap with an intricate spiral feature. Some of the materials that fulfill these criteria are ZrO_2, Macor®, boron nitride, Kel-F®, Vespel®, and Torlon®. Among these choices, ZrO_2 and Vespel are popular materials for the drive cap because ZrO_2 has superior mechanical strength and a low thermal expansion coefficient, which is preferred for low-temperature dynamic nuclear polarization (DNP) experiments [6–8]. However, machining ZrO_2 is challenging and, hence, expensive, i.e. a 3.2 mm ZrO_2 cap costs ~ 1 k USD (CortecNet). Although the Vespel drive cap is more affordable (~130 USD for 3.2 mm), it is still a non-negligible expense because the delicate fins on the drive cap wear out easily if they are mishandled

* Corresponding author at: Laboratoire des Biomolécules, LBM, Département de Chimie, École Normale Supérieure, PSL University, Sorbonne Université, CNRS, 75005 Paris, France.
E-mail address: kong-ooi.tan@ens.psl.eu (K.O. Tan).
[1] Denotes equal contributions.

https://doi.org/10.1016/j.jmr.2023.107391
1090-7807/

Table 1
Summary of rotor sizes, spinning frequencies, and other specifications of both commercial (Vespel) and 3D-printed MAS drive caps. We have tested at least 10 pieces for each rotor size, except for the industrial-printed (BMF) 1.3 mm drive cap, where only two out of three available pieces were tested. We have only examined the 3.2 mm cap at ~ 100 K only once for ~ 17 h. RT refers to room temperature.

Diameter (mm)	Volume (μl)	Max ν_r of machined Vespel cap (kHz)	Max ν_r of 3D-printed cap (kHz)	Printing consistency
7	240	7	6 kHz ± 0.5 Hz	<100 %
4	70	15	10 kHz ± 1.6 Hz (Elegoo, no hole) 7 kHz ± 0.3 Hz (Elegoo, with hole)	<100 %
3.2	30	24 (RT) 12 (~100 K)	22 kHz ± 1.3 Hz. (RT) 8 kHz ± 2 Hz (~100 K)	<100 %
2.5	12	35	26 kHz ± 2.1 Hz	95 %
1.3	2.5	67	46 kHz ± 1.1 Hz (Form 3+) 60 kHz ± 3.4 Hz (BMF)	92 %

or after repeatedly fitted/removed from the rotor. These effects are noticeably noted for smaller rotors, i.e., the 0.7 mm drive cap is usually for one-time use only, and it has to be replaced with a new piece when packing new samples into the same rotor. To minimize the expenditure on these consumables (MAS drive caps), it has been recently demonstrated that the MAS drive caps can be fabricated using relatively low-cost 3D printing technology [9,10].

There are two main categories of 3D printing technology: fused deposition modelling (FDM) and stereolithography (SLA). Although the FDM method has, in general, a poorer resolution, it is more affordable and easier to use relative to the resin-based SLA method. Both 3D printing technologies have been exploited in various NMR applications, ranging from fabricating MAS sample eject systems [11], RF coils [12–15], NMR sample tubes [16], parahydrogen generator [17], NMR sample degassing apparatus [18,19], NMR probeheads [20], etc. Besides these examples, Xu et al. have recently demonstrated that it is possible to fabricate MAS stator and drive caps using FDM, but only for > 3.5 mm system [9]. High-resolution SLA technology has also been exploited for constructing MAS spinning system. Notable examples include the fabrication of > 4 mm spherical-rotor stators using a benchtop 3D printer by the Barnes' group [21,22], and a 3.2 mm cylindrical-rotor stator and drive caps produced by dedicated manufacturing companies reported by Banks et al. [10]. Although outsourcing the manufacturing process can save labour resources, we note that the quality of the parts varies across different batches. This could be because the printing and/or post-processing steps performed by the company are not necessarily the same for each batch. Consequently, the lack of consistent results could lead to a more time- and cost-consuming process. Moreover, the same publication commented that the benchtop 3D printer (Form 3 with 25 μm XY resolution) was tested to be incapable of producing the 3.2 mm drive caps [10]. In this publication, we re-examine this statement by showing that not only the Form 3+ 3D printer can fabricate robust 3.2 mm drive caps, but also smaller 2.5- and 1.3-mm drive caps (with slightly compromised performances). In particular, the 3.2 mm 3D-printed drive caps (Fig. 1) can spin up to $\nu_r = 22$ kHz ± 1.3 Hz (Table 1), which has similar performances as the commercial versions, but only costs < 1 US cents and 5 min/-piece to be 3D-printed (assuming a simultaneous printing of 100 pieces in a single print job). Additionally, the in-house fabricated 3D-printed drive caps exhibit excellent spinning stability that is sufficient for practical multi-dimensional MAS NMR experiments.

2. Experimental methods

2.1. 3D printing and Post-Processing methods

The drive caps were designed in Autodesk Inventor (Autodesk Inc, San Rafael) following a similar design described in Banks et al. [10]. The drive caps were printed using standard Clear v4 resin in a Form 3+ (Formlabs) printer with a 25 μm XY resolution and layer thickness. The 3D printer costs ~ 4 k USD, and the resin costs ~ 140 USD/litre. The printing supports were placed on the bottom of the stem with a contact point size of 0.3 mm. It takes ~ 4 h to simultaneously 3D-print 100 pieces of drive caps in a single print job. Note that the build platform of the 3D printer can accommodate >100 pieces in a single print (if needed) without significantly increasing the printing hours. After the printing job finished, the parts were first rinsed in an isopropanol-water mix-

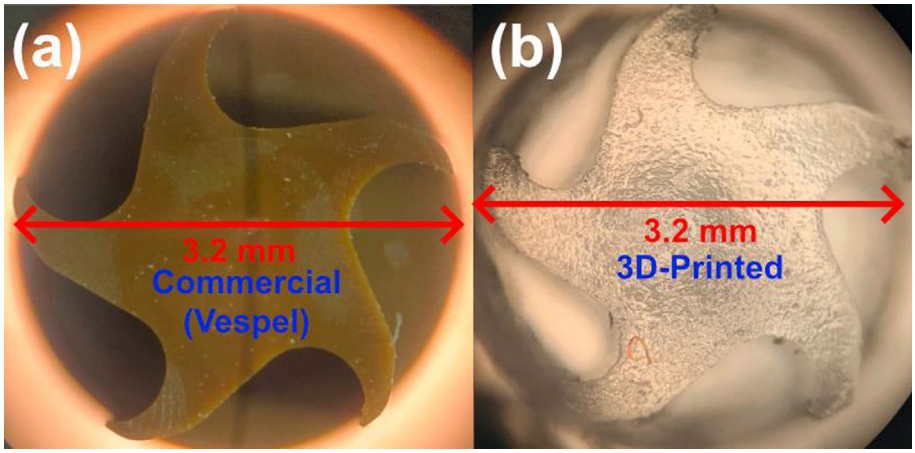

Fig. 1. Image of (**a**) a commercial (Bruker) Vespel and (**b**) a 3D-printed 3.2 mm MAS drive cap.

ture (9:1 by volume ratio) to remove the uncured resin and irregularities on the surface. Then, the supports were removed and rinsed again before being cured under UV light (Elegoo Mercury) for 1 h (2x30 min, with another rinsing step between the two curing sessions) to enhance the mechanical properties. Note that the caps should be completely dry after every rinsing step. It is known that the SLA-printed parts gradually shrink in size over time, and the long curing time (1 hr) is a crucial step to accelerate the shrinking process and, hence, more stable in the long term. To account for the change in dimension after the post-processing steps, we have iteratively compensated for the changes by redesigning and reprinting the parts. In addition to the Form 3+ 3D printer, we have also tested another benchtop 3D printer (Elegoo Saturn), which has a lower XY resolution (50 μm). We have used the Elegoo 3D printer to print 4 mm caps (with Elegoo standard grey resin), and they show similar performances as the commercial (Bruker) version.

2.2. *Artefact* compensation *by iterative design modification*

Note that the dimensions of the 3D-printed pieces could be slightly different from the computer-aided design (CAD) due to the properties of the resins, printing environment (temperature), post-processing steps, printing orientations, etc. Nevertheless, some of these undesired changes could be compensated by minor modifications (often iterative) in the CAD. An example of this is the 'overhang' feature that occurs when the resin tends to bulge downward due to gravity (Fig. 2**a**). The artefact has resulted in a small gap between the drive cap and the rotor and, hence, compromised the spinning performances, i.e., it does not spin up beyond 22 kHz. Although this feature can be partially compensated by reversing the printing orientation, it, unfortunately, affects the form of the fins (Fig. 2**b**). Thus, we introduced a concave curvature to the horizontal slab (Fig. 2**c**). Consequently, the printed part (Fig. 2**d**) did result in a better fit and a higher spinning frequency to $\sim$ 26 kHz. Besides that, we have also made the fins on the 1.3 mm drive cap sharper (Fig. 3**d and e**) to compensate for the broader-than-expected fins (Fig. 3**a and b**) due to the finite size of the laser beam used in the Form 3+ 3D printer (85 μm). The corrected drive caps (Fig. 3**e**) were able to achieve the same spinning frequency with less drive gas (vide infra, Fig. 6**a**), and the maximum ν_r was improved from 37 to 45 kHz. Additionally, we would like to highlight that the diameters of the stem (the component that fits into the rotor) and the slab (Fig. 2**c**) of the drive caps require very tight tolerances, i.e., they must be fabricated within

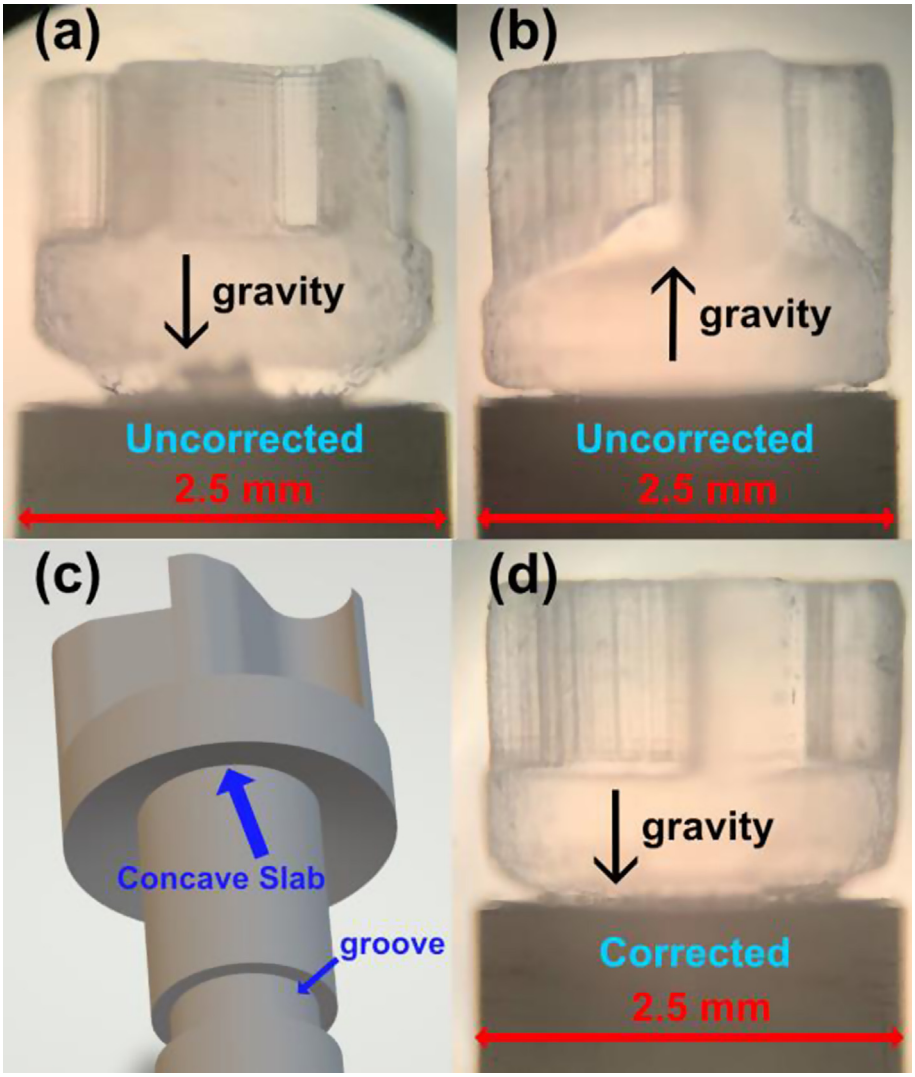

Fig. 2. Images of 2.5 mm MAS drive caps. Note the undesirable overhang effect present in the (**a**) upright and (**b**) reversed orientation. The artefacts were compensated by designing (**c**) a concaved (curved inward) slab, which yields the (**d**) corrected cap that improves the maximum spinning frequency from 22 to 26 kHz.

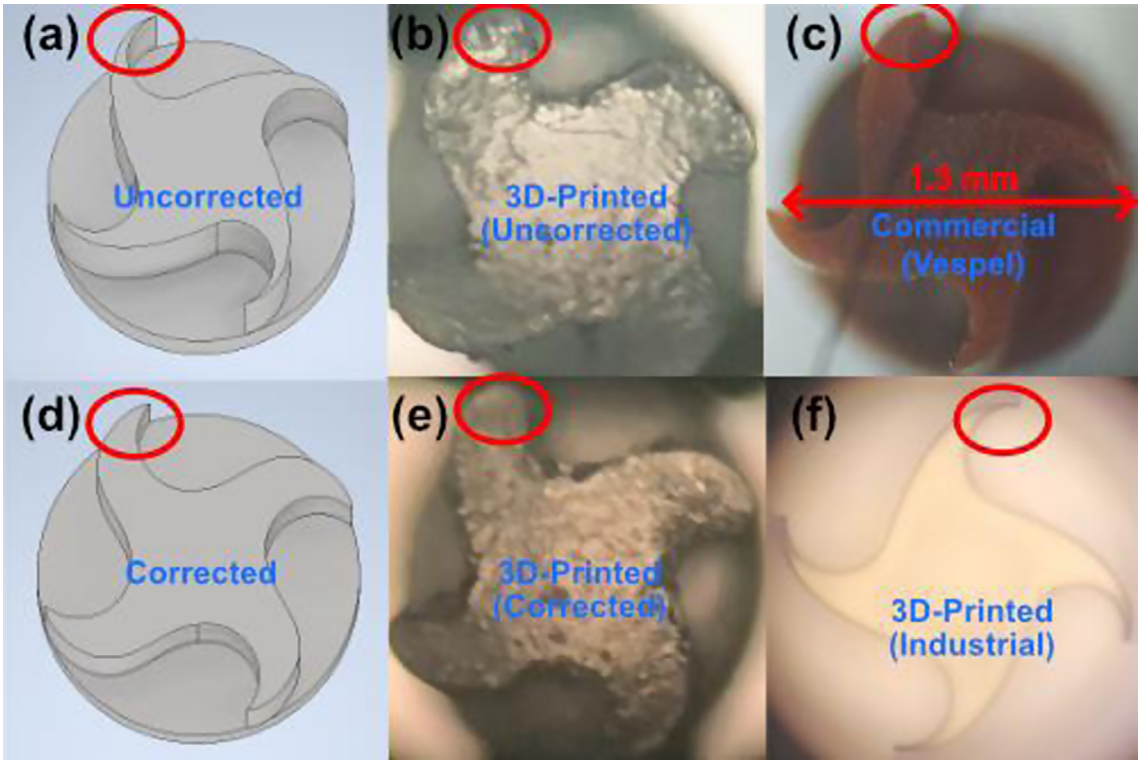

Fig. 3. 1.3 mm MAS drive caps. Images of the (**a** and **d**) CAD and (**b** and **e**) 3D-printed pieces (**a** and **b**) before and (**d** and **e**) after the design compensation. Images of the (**c**) machined and (**f**) industrial 3D-printed (BMF) drive caps.

a ~ 10 μm accuracy for optimal performances. At last, we emphasize that such iterative compensation is possible only because the 3D printing protocol yields very consistent and reproducible results. We have fabricated many batches of the drive caps over several months, and they yield very similar results.

2.3. MAS *experiments using 3D-Printed caps*

The 3D-printed caps were fitted into standard ZrO_2 rotors for MAS experiments in Bruker MAS probes or a benchtop spinning station at ambient temperature. A Bruker MAS II unit was used to regulate the drive and bearing gas pressure to achieve a stable spinning frequency. We have tested at least 10 pieces of each design for at least 15 min to evaluate the MAS performance. The pressure of each gas inlet and spinning frequency as a function of time in the automated mode were logged using TopSpin (Bruker). We have tested the 3.2 mm drive caps on both ZrO_2 and sapphire rotors. All zirconia rotors fitted with 3D-printed caps spun > 20 kHz without major issues. However, the sapphire rotor crashed when spun above 18 kHz (rated for 15 kHz at RT). For the 1.3 mm drive caps printed with an industrial 3D printer (Boston Micro Fabrication (BMF)), we have tested only 2 out of the 3 ordered pieces.

2.4. *NMR samples and experiments*

The ^{13}C-^{15}N L-Isoleucine sample was purchased from CortecNet and used without further purification. For the Metal-Organic Framework (MOF-801) sample [23], the MOF was synthesized through an established procedure and washed with D_2O using ultrasounds [23]. The D_2O washing step was performed to promote an exchange of the hydroxyl proton (Zr-OH) with deuterium, which helps unambiguously assign the Zr-O^{1}H NMR peak observed in an H_2O-washed MOF sample. The D_2O-washed MOF sample was then activated in a vacuum drying oven for 12 h at 100 °C to remove excess solvent. To minimize the exposure of the dried MOF sample to the moist in the atmosphere, the sample was packed into a 3.2 mm rotor closed with a 3D-printed drive cap sealed with silicone-filled (Bluestar CAF 1) groove inside an argon-filled glove box.

The NMR spectra were acquired using an 800 MHz spectrometer equipped with an Avance Neo console (Bruker). We have used either a 1.3 mm, 2.5 mm, or 3.2 mm (E-free) triple-channel MAS probe to perform MAS NMR experiments. The ^1H and ^{13}C chemical shifts were referenced to the adamantane signal at 38.5 ppm on the tetramethylsilane (TMS) scale. The RFDR experiment (Fig. 4**a**) was performed using the 1.3 mm probe at 45 kHz MAS frequency with a ~ 2 ms RFDR mixing time. The DARR experiment (Fig. 4**b**) was performed using the 2.5 mm probe at ν_r = 20 kHz with a 100 ms DARR mixing time. The HETCOR spectra (Fig. 4**c & d**) were acquired using a 3.2 mm probe at ν_r = 10 kHz. The experimental time for each 2D experiment is ~ 2 hr. The magic angle and field B_0 homogeneity were optimized with KBr and adamantane, respectively. The low-temperature MAS experiment (Fig. 7) was performed using a 3.2 mm HXY MAS DNP probe (Bruker). The sapphire rotor was packed with MOF-801, the surface of which was wetted with solutions of DNP juice (d_8-glycerol: D_2O: H_2O in 6:3:1 by volume) doped with 5 mM TinyPol. We filled the groove on the 3D-printed drive cap with red silicone sealant so that the cap does not become loose as it shrinks at low temperatures [11]. Prior to the MAS experiment, the rotor was immersed in liquid nitrogen at ~ 77 K to ensure that the 3D-printed cap remained intact and well-fitted to the rotor. We initially planned to perform DNP experiments with the 3.2 mm system, but the gyrotron was not operational during the experiment. Nevertheless, we performed conventional NMR experiments at low temperatures without microwaves, which allows the sample to reach a colder temperature (~105 K) due to the absence of microwave heating. The stator temperature was maintained at ~ 109 K (measured at

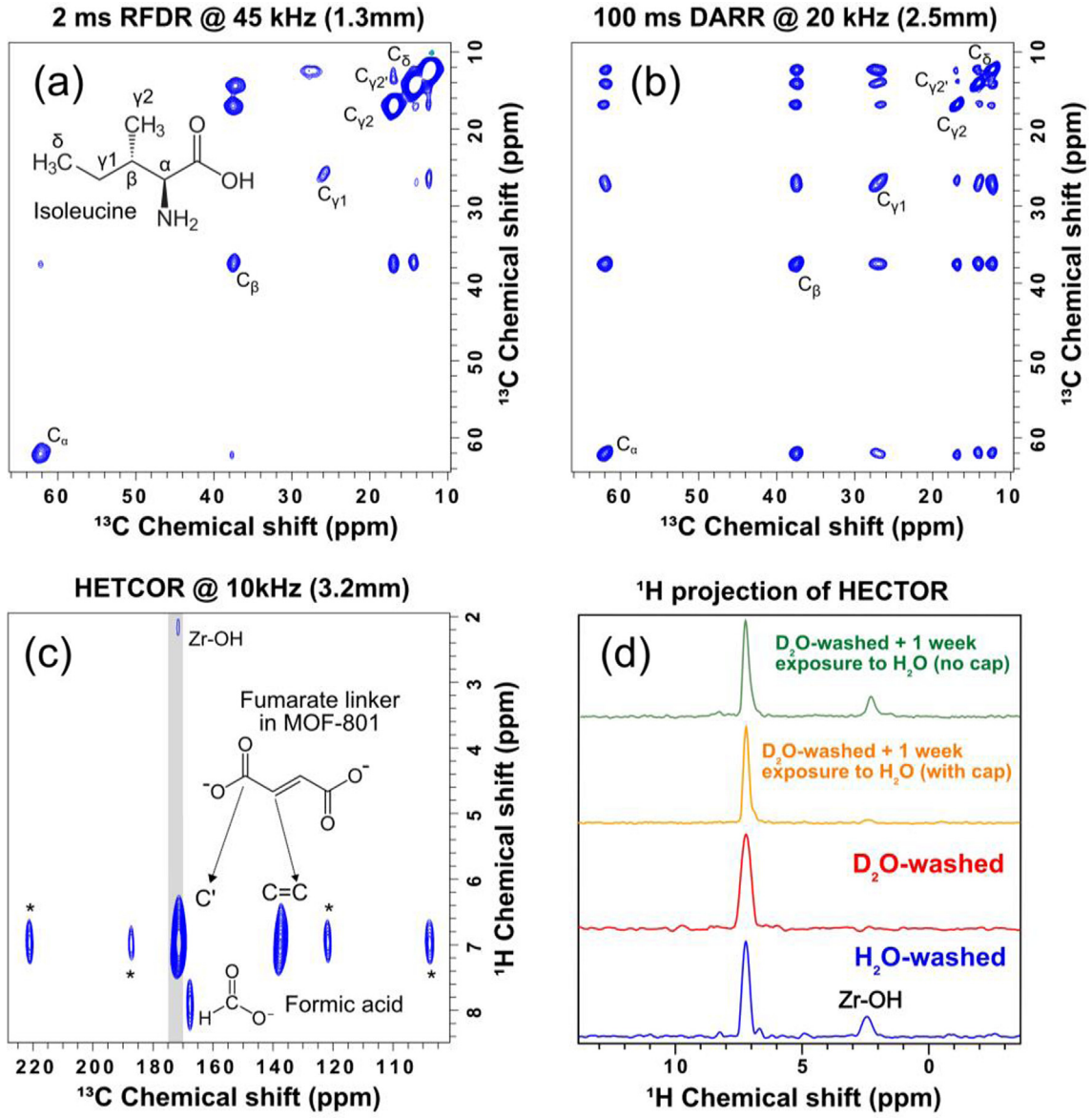

Fig. 4. 2D NMR spectra acquired with (**a**) 1.3 mm, (**b**) 2.5 mm, or (**c**) 3.2 mm 3D-printed caps. (**a**) ^{13}C–^{13}C RFDR spectrum of L-Isoleucine in a 1.3 mm rotor at ν_r = 45 kHz. (**b**) ^{13}C–^{13}C DARR spectrum of L-Isoleucine in a 2.5 mm rotor with ν_r = 20 kHz. (**c**) ^{1}H–^{13}C HETCOR spectrum of MOF-801 in a 3.2 mm rotor with ν_r = 10 kHz. * denotes the spinning sidebands. Note that there are two isoleucine isomers that give rise to two $C_{\gamma 2}$ peaks, where the second peak is labelled as $C_{\gamma 2'}$ [39]. (**d**) 1D projection showing the ^{1}H dimension (integrate along the grey area in (**c**)) for MOF-801 washed in H_2O (blue), D_2O (red), D_2O-washed MOF exposed to saturated water vapour for one week with (yellow) or without (green) the 3D-printed cap sealed with silicone. (For interpretation of the references to colour in this figure legend, the reader is referred to the web version of this article.)

stator after the mixing of the variable temperature (VT), bearing, and drive gas) by regulating the temperature of the three spinning gases at the probe base to be ~ 95 K. Hence, we estimated the actual sample temperature to be ~ 100 K.

3. Results and discussions

A statistical summary of the MAS tests performed on the 1.3 to 7 mm drive caps is tabulated in Table 1. The max ν_r is defined as the maximum spinning frequency we have tested, and it is intentionally chosen to be slightly below the specification of the commercial (Bruker) caps to avoid rotor-crash incidents. We found that the in-house 3D-printed drive caps for sizes ≥ 3.2 mm have almost equivalent MAS performances as the commercial caps, while the cost of 3D printing is almost negligible. Nevertheless, the smaller 3D-printed drive caps (1.3 mm and 2.5 mm) yield less satisfactory spinning performances than the machined caps. Hence, we improvised the original CAD to compensate for the printing inaccuracies (vide supra), which moderately improved the maximum ν_r to > 70 % of those specified for the commercial caps, i.e., the 2.5- and 1.3-mm 3D-printed caps can spin up to 26 and 46 kHz, respectively. Despite the lower max ν_r, the 3D-printed caps still achieve excellent spinning stability (≤ 2 Hz), which is practical for MAS NMR experiments.

To further assess the transfer efficiency of the momentum from the gas to the printed drive, we have recorded the spinning profiles (Fig. 6) of the smaller caps as a function of the drive gas pressure. We noted that the 3D-printed 1.3 mm caps are less efficient and require more drive gas to reach the same spinning frequency as the commercial caps [24,25]. We hyphothesized that the 1.3 mm caps could spin faster if they could be more accurately made. To test our hyphothesis, we have 3D-printed the 1.3 mm caps using

a state-of-the-art industrial 3D printer (BMF) with HTL resin, which has a ~ 12x higher XY resolution (2 μm) than our desktop Form 3+ printer. Not only the BMF cap exhibits sharper fins (circled in Fig. 3**f**) than those made by Form 3+ (Fig. 3**e**), but also those machined Vespel caps (Fig. 3**c**). Indeed, those industrial-printed caps were able to achieve ν_r = 60 kHz ± 3 Hz (Fig. 5**b**). Note that we have only tested two out of three available pieces. Both pieces achieve similar spinning frequencies with the same bearing and drive gas, but the second piece broke when spun above 50 kHz. This issue could be mitigated if harder materials (alumina ceramics or *HT 200* from BMF) are used for printing the caps, but they are not in-house fabricated and are beyond the scope of this work. Although these industrial 3D-printed caps cost > 20 USD / piece (for a large-quantity order), they are still an order of magnitude cheaper than the machined Vespel caps.

On the printing consistency, which we defined as the ratio of the number of pieces that spin to the total number of printed parts, we have achieved very consistent results, i.e., all printed drive caps can be reliably reproduced with > 90 % consistency. Note that it is necessary to spin-test the printed drive caps ≤ 2.5 mm, as the defective pieces cannot be easily identified with visible features. For ≥ 3.2 mm drive caps, the consistencies are remarkably near 100 %. For the most used 3.2 mm system, we have repeatedly fabricated >100 pieces over a few months using the same optimized protocol, and they have all worked. We have also tested both freshly printed and several-month-old pieces, and they yield equal

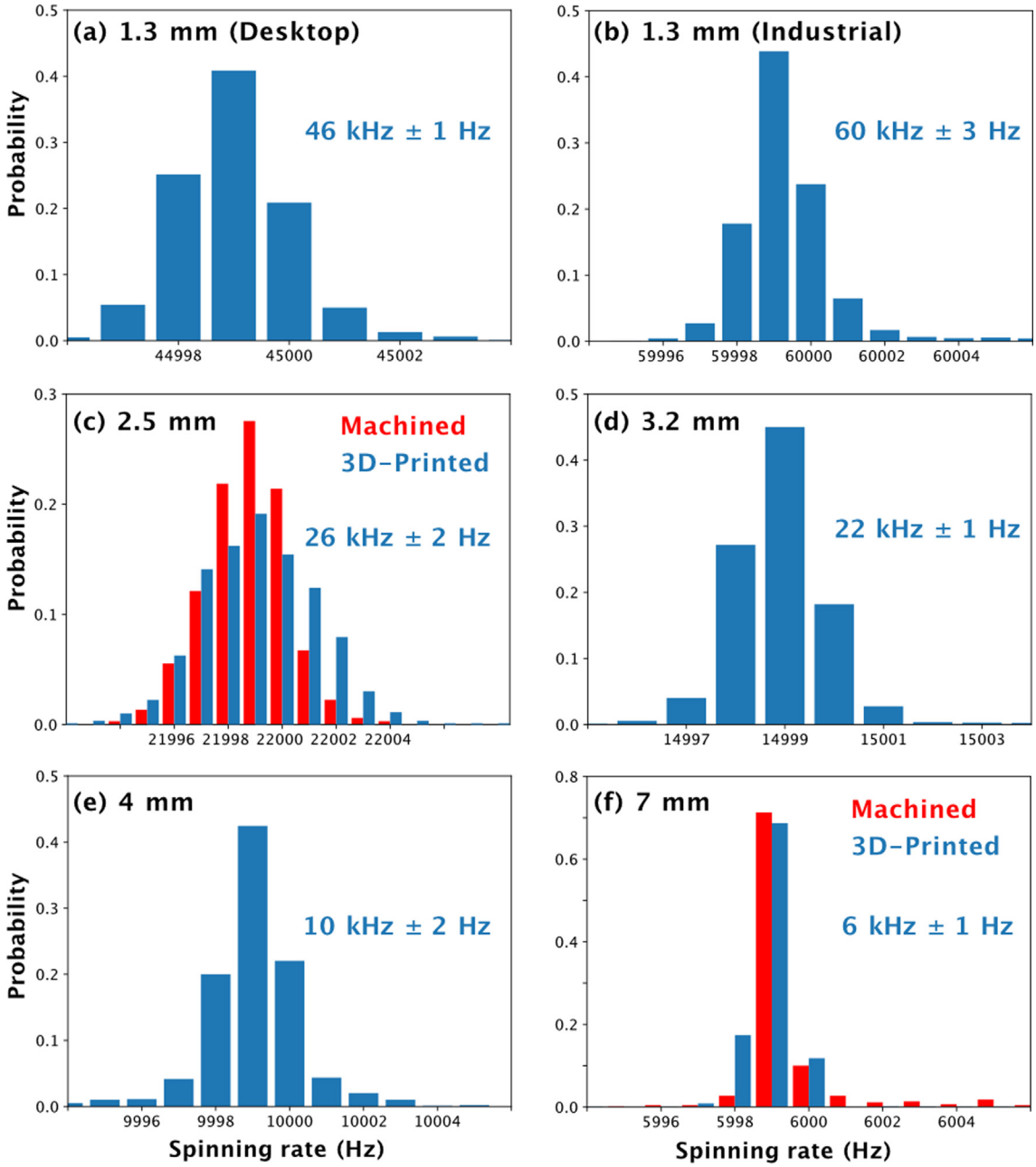

Fig. 5. Histograms of MAS frequencies for (**a** and **b**) 1.3 mm, (**c**) 2.5 mm, (**d**) 3.2 mm, (**e**) 4 mm, and (**f**) 7 mm drive caps that are either 3D-printed (blue) or machined (red, Bruker). All 3D-printed caps were made in-house except (**b**), which was outsourced to BMF. All caps were tested in a regulated mode using MAS II for at least 15 min. Only the standard deviation in MAS frequency for the 3D-printed caps is shown. The results are summarized in Table 1. (For interpretation of the references to colour in this figure legend, the reader is referred to the web version of this article.)

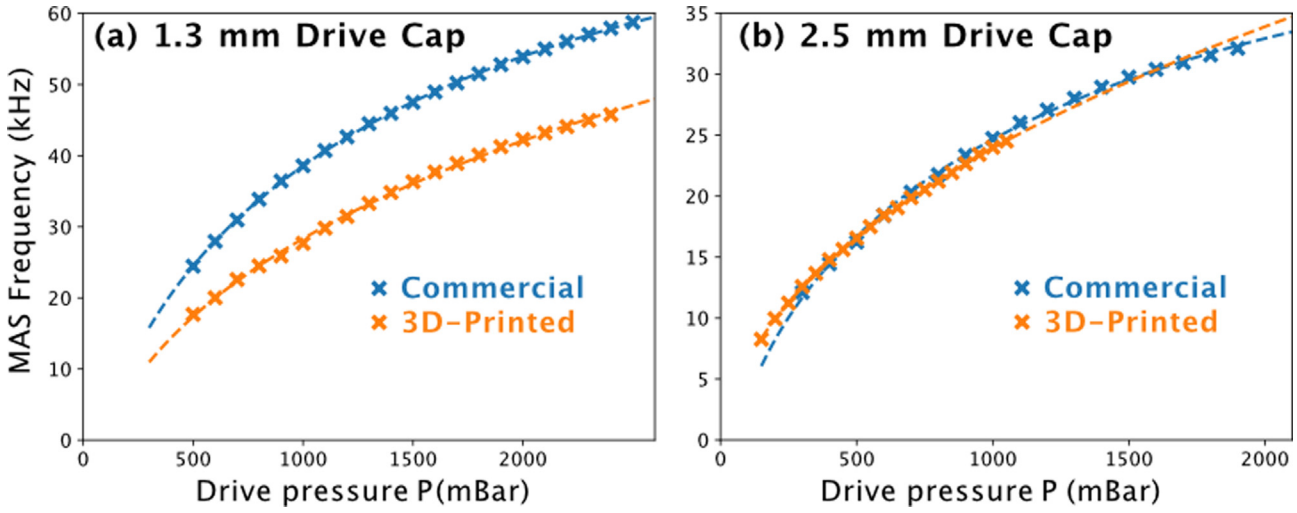

Fig. 6. MAS frequencies of the (**a**) 1.3 mm and (**b**) 2.5 mm drive caps as a function of the drive gas pressure with a constant bearing gas pressure of 3 bar. The dashed lines (–) show fitted data with function $\nu_r = AP + B\sqrt{P} + C$, where A, B, and C are numerical constants.

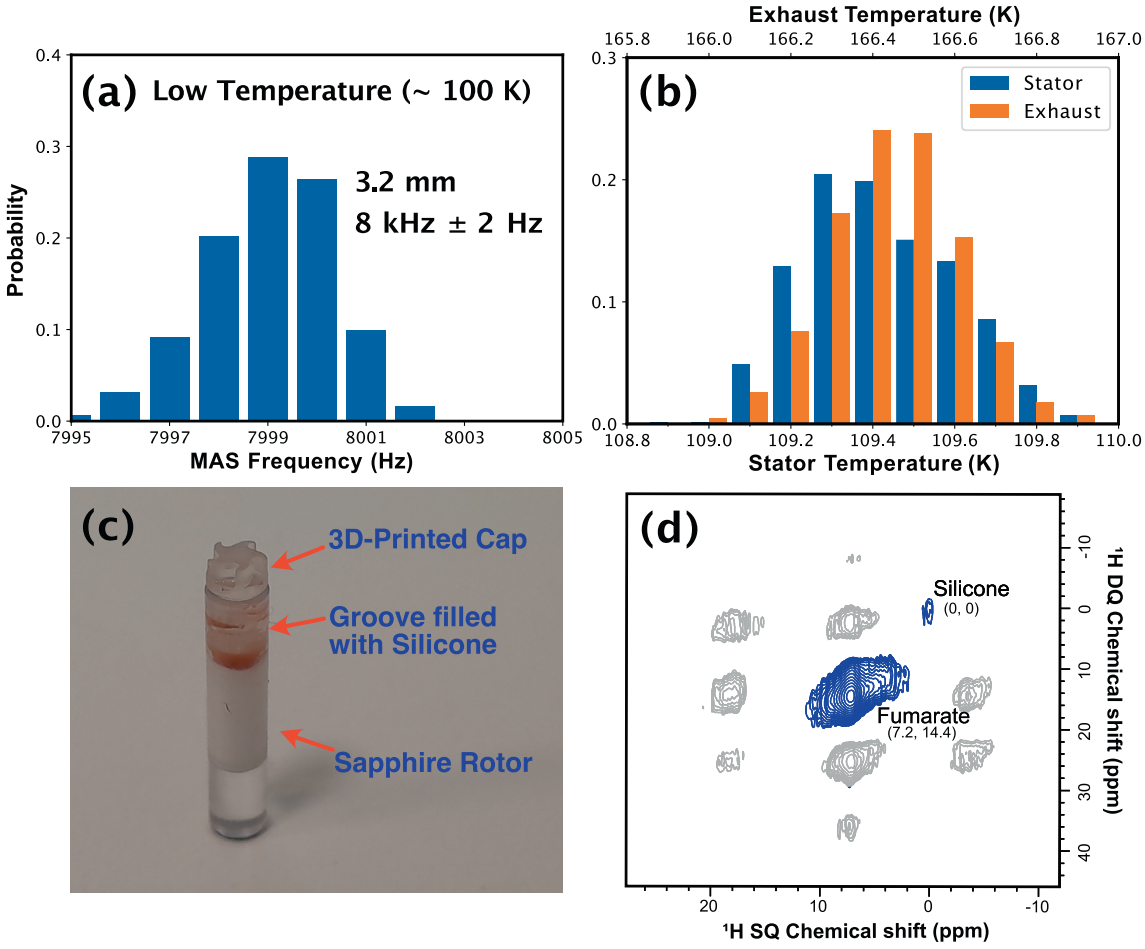

Fig. 7. (**a**) Histogram of MAS frequency of a 3.2 mm 3D-printed drive cap at ~ 100 K. (**b**) The stator and exhaust temperature were measured to be ~ 109.4 K and ~ 166.5 K, respectively. The exhaust temperature was measured at the probe base. (**c**) Photo of a 3D-printed drive cap with a silicone-filled groove to prevent the cap from becoming loose at low temperatures. (**d**) A 2D ^{1}H–^{1}H DQ-SQ (single quantum) spectrum was acquired with a C7 sequence at ~ 100 K and 18.8 T. As the exact chemical composition of the commercial silicone sealant is not known, we tentatively assign the anomalous peak to originate from the silicone sealant. In the 2D spectrum, we have observed peaks of both silicone and ligands of MOF 801 (fumarate) but not a correlation between the two sites.

performances. It is noteworthy to be aware that we did not reuse any old caps because the cost is almost negligible.

To assess if the 3D-printed drive caps are practical for long MAS NMR experiments, we have performed various 2D NMR correlation experiments on the 1.3 mm, 2.5 mm, and 3.2 mm drive caps on standard compounds. Among these experiments, the RFDR dipolar recoupling experiment performed on the 1.3 mm rotor requires the rf pulses to be rotor-synchronized to yield an efficient correlation

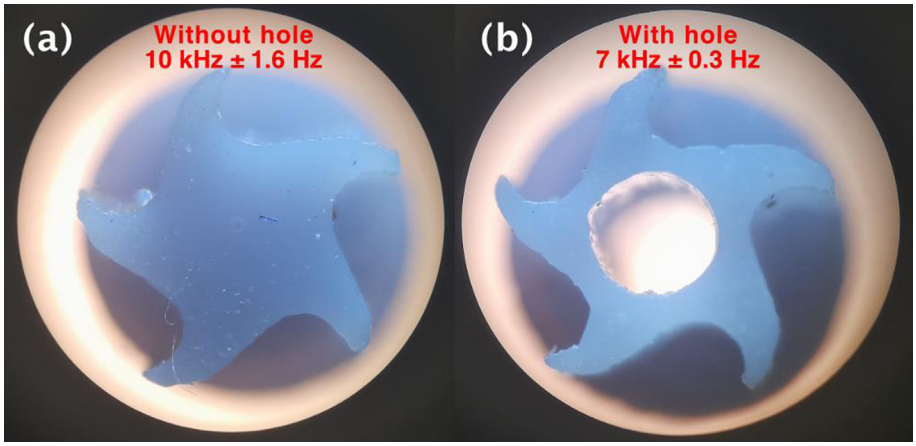

Fig. 8. Image of the 4 mm drive cap (**a**) without or (**b**) with a center hole. The drive caps were printed using a desktop 3D printer (Elegoo Saturn). Their MAS performances are specified in the image.

between the ^{13}C peaks [26]. The fact that the 2D spectra show excellent linewidths and all the expected cross peaks, we conclude that the homebuilt 3D-printed drive caps are practical for actual MAS NMR experiments.

In addition to the standard drive cap designs, we also prototyped new models that could be useful for special NMR applications. For instance, we have added a groove to the stem (Fig. 2**c**) so that the rotor could be sealed using epoxy or silicone sealant, which is useful for studying air- or moisture-sensitive NMR samples. As proof of principle, we have applied such a protocol on a MOF-801 sample packed in a 3.2 mm rotor (see **Section 2.4**). MOF-801 is built-up from $Zr_6O_4(OH)_4$ oxo-clusters and fumaric acid molecules. The labile proton in the –OH groups could, in principle, exchange with deuterium. To test the hypothesis, we recorded some 2D ^{1}H–^{13}C HETCOR spectra (Fig. 4**c & d**) of MOF-801 prepared under various conditions. The ^{1}H peak intensity at ~ 2.4 ppm is significantly lower than in the D_2O-washed sample relative to the H_2O-washed counterpart. This implies that labile ^{1}H in Zr-OH could be exchanged with D_2O to form Zr-OD, which attenuates the ^{1}H peak intensity. The experimental results allow us to unambiguously assign the observed ^{1}H peak to Zr-OH, which was previously stated in literature with only DFT calculations [27]. To examine if the sealed 3D-printed cap is sufficiently robust for studying moisture-sensitive samples, we put the rotors packed with D_2O-washed samples inside Eppendorf vials filled with a few drops of H_2O for ~ 1 week. For the rotor fitted with a silicone-sealed 3D-printed cap, the HETCOR spectrum (Fig. 4**d**) is nearly identical to the spectrum acquired before exposure to water vapor. In contrast, the rotor without a cap showed significant growth in the Zr-O^{1}H peak. Hence, the results confirm that the 3D-printed cap with silicone seals provides a robust airtight condition suitable for studying air- or moisture-sensitive NMR samples. Moreover, emptying the rotors fitted with silicone- or epoxy-sealed drive caps—which could become unusable if destructively removed—is more cost-efficient if the caps were 3D-printed in-house.

Another main concern about the 3D-printed drive caps is their feasibility for low-temperature applications. It was reported by Banks et al. that the 3D-printed caps fabricated by an industrial 3D printer (Protolabs) crack at ~ 100 K [10]. To examine our printed drive caps printed (Formlabs), we fitted a 3D-printed cap into a sapphire rotor packed with MOF-801 wetted with DNP juice (see Experimental Section) and sealed with silicone sealant (Fig. 7**c**), before spinning it at ~ 100 K using a 3.2 mm 800 MHz MAS DNP probe. Fig. 7**a** shows the histogram of regulated MAS frequency of ν_r = 8 kHz ± 2 Hz at a sample temperature of ~ 100 K over ~ 17 h. The recorded spinning frequency at low temperatures is slightly less stable than the room-temperature operation (Fig. 5**d**), possibly due to a larger standard deviation in stator temperature (see Fig. 7**b** and Experimental Section). Following that, we recorded a 2D ^{1}H–^{1}H double-quantum filtered (DQF) spectrum (Fig. 7**d**) using a symmetry-based $C7_2^1$ sequence, which is a rotor-synchronized dipolar recoupling sequence that requires a stable spinning frequency for efficient performance [28]. The 2D experiment acquired at ~ 100 K demonstrates that the 3D-printed drive cap is robust for low-temperature (including MAS DNP) applications.

Besides that, we have also modelled 4 mm drive caps with a center hole (Fig. 8), which could be useful for in-situ monitoring of chemical reactions during MAS experiments, or those NMR experiments that require in-situ illumination of light or lasers [29–32]. For the first case, similar instrumentation and experiments were demonstrated in the literature [33–36], where a reactant gas was directed into a 7 mm rotor via an injection tube through the drive cap with an axial hole. The 4 mm drive cap (without an injection tube) could spin till ν_r = 7 kHz ± 0.3 Hz, which is slightly slower than the normal cap (~ 10 kHz).

4. Conclusion

We have demonstrated that it is possible to fabricate 1.3–7 mm drive caps using an affordable desktop 3D printer in-house. The moderate-accuracy but high-precision 3D printing method allows us to fabricate highly consistent (> 90 %) MAS drive caps with similar results as the commercial caps for the ≥ 3.2 mm system. The smaller (≤ 2.5 mm) caps can spin up to ~ 70 % as fast as the commercial caps, and yet with a high spinning stability (≤ 2 Hz). The high spinning stability of the drive caps allows practical multidimensional NMR experiments to be performed. Additionally, we have exploited the high-resolution (2 μm) industrial 3D printer (BMF) to fabricate the 1.3 mm caps, which yield near equivalent MAS performances as the commercial caps. We foresee that it could be possible to 3D print smaller (≤ 0.7 mm) [4,5,37,38] caps with similar or harder materials offered by the same company. In contrast to traditional machining, which becomes more challenging and expensive to fabricate smaller drive caps, 3D printing becomes cheaper as the size of the drive cap decreases—because more pieces could be simultaneously printed in a single print job on the platform. The relatively low cost and short fabrication time have allowed us to prototype new designs for new or custom MAS NMR applications. For instance, it costs < 1 USD and 6 h to fabricate

100 pieces of the MAS drive caps in-house. Not only does the silicone-filled groove on the 3D-printed cap provides an airtight environment suitable for studying air- or moisture-sensitive materials, but also allows low-temperature MAS experiment (including DNP) at $\sim$ 100 K. As the 3D printing technology continues to flourish, we expect higher-resolution 3D printers will become more easily accessible by laboratories, and new tools could be fabricated in-house for novel NMR experiments.

Data availability

Data will be made available on request.

Declaration of Competing Interest

The authors declare that they have no known competing financial interests or personal relationships that could have appeared to influence the work reported in this paper.

Acknowledgements

We acknowledge Dr. Nicolas Birlirakis, Dr. Dan Banks, and Natalie Golota for helpful discussions. This work was supported by fundings obtained from the French National Research Agency (ANR): *PulsedDNP* (ANR-20-ERC9-0008) and *HFPulsedDNP* (ANR-21-CE29-0019), as well as RESPORE (n° 339299). Wenqing Lu acknowledges the China Scholarship Council for providing the funding (n° 201906880002).

Appendix A. Supplementary material

Supplementary data to this article can be found online at https://doi.org/10.1016/j.jmr.2023.107391.

References

[1] B. Reif, S.E. Ashbrook, L. Emsley, M. Hong, Nat. Rev. Methods Prim. 1 (2021) 2.
[2] E.R. Andrew, A. Bradbury, R.G. Eades, Nature 182 (1958) 1659.
[3] I.J. Lowe, Phys. Rev. Lett. 2 (1959) 285.
[4] M. Schledorn, A.A. Malär, A. Torosyan, S. Penzel, D. Klose, A. Oss, M. Org, S. Wang, L. Lecoq, R. Cadalbert, A. Samoson, A. Böckmann, B.H. Meier, ChemBioChem 21 (2020) 2540.
[5] A. Böckmann, M. Ernst, B.H. Meier, J. Magn. Reson. 253 (2015) 71.
[6] F.D. Doty, EMagRes (2007).
[7] F.D. Doty, P.D. Ellis, Rev. Sci. Instrum. 52 (1981) 1868.
[8] N. Herzog, A. Weber, A. Purea, D. Osen, B. Knott, F. Engelke, D. Wilhelm, J. Fluids Eng. 144 (2022).
[9] K. Xu, O. Pecher, M. Braun, J. Schmedt auf der Günne, J. Magn. Reson. 333 (2021).
[10] D. Banks, B. Michael, N. Golota, R.G. Griffin, J. Magn. Reson. 335 (2022).
[11] A.B. Barnes, M.L. Mak-Jurkauskas, Y. Matsuki, V.S. Bajaj, P.C.A. van der Wel, R. DeRocher, J. Bryant, J.R. Sirigiri, R.J. Temkin, J. Lugtenburg, J. Herzfeld, R.G. Griffin, J. Magn. Reson. 198 (2009) 261.
[12] J.I. Kelz, J.E. Kelly, R.W. Martin, J. Magn. Reson. 305 (2019) 89.
[13] H. Vanduffel, C. Parra-Cabrera, W. Gsell, R. Oliveira-Silva, L. Goossens, R. Peeters, U. Himmelreich, B. Van Hooreweder, D. Sakellariou, W. Vanduffel, R. Ameloot, Adv. Mater. Technol. 2200647 (2022) 2200647.
[14] J.I. Kelz, J.L. Uribe, R.W. Martin, J. Magn. Reson. Open 6–7 (2021).
[15] S.J. Elliott, M. Ceillier, O. Cala, Q. Stern, S.F. Cousin, S. Jannin, J. Magn. Reson. Open 10–11 (2022).
[16] Z. Long, J. Ruthford, S.J. Opella, J. Magn. Reson. 327 (2021).
[17] F. Ellermann, A. Pravdivtsev, J.-B. Hövener, Magn. Reson. 2 (2021) 49.
[18] L. Delage-Laurin, R.S. Palani, N. Golota, M. Mardini, Y. Ouyang, K.O. Tan, T.M. Swager, R.G. Griffin, J. Am. Chem. Soc. 143 (2021) 20281.
[19] K.O. Tan, L. Yang, M. Mardini, C.B. Cheong, B. Driesschaert, M. Dincă, R.G. Griffin, Chem. – A Eur. J. 13 (2022) 287.
[20] J. Xie, X. You, Y. Huang, Z. Ni, X. Wang, X. Li, C. Yang, D. Zhang, H. Chen, H. Sun, Z. Chen, Nat. Commun. 11 (2020) 1.
[21] P. Chen, B.J. Albert, C. Gao, N. Alaniva, L.E. Price, F.J. Scott, E.P. Saliba, E.L. Sesti, P.T. Judge, E.W. Fisher, A.B. Barnes, Sci. Adv. 4 (2018) eaau1540.
[22] C. Gao, P.T. Judge, E.L. Sesti, L.E. Price, N. Alaniva, E.P. Saliba, B.J. Albert, N.J. Soper, P.-H. Chen, A.B. Barnes, J. Magn. Reson. (2019).
[23] H. Furukawa, F. Gándara, Y.-B. Zhang, J. Jiang, W.L. Queen, M.R. Hudson, O.M. Yaghi, J. Am. Chem. Soc. 136 (2014) 4369.
[24] D. Wilhelm, A. Purea, F. Engelke, J. Magn. Reson. 257 (2015) 51.
[25] N. Herzog, D. Wilhelm, S. Koch, A. Purea, D. Osen, B. Knott, F. Engelke, J. Fluids Eng. 138 (2016) 1.
[26] A.E. Bennett, R.G. Griffin, J.H. Ok, S. Vega, J. Chem. Phys. 96 (1992) 8624.
[27] S. Devautour-Vinot, G. Maurin, C. Serre, P. Horcajada, D. Paula da Cunha, V. Guillerm, E. de Souza Costa, F. Taulelle, C. Martineau, Chem. Mater. 24 (2012) 2168.
[28] M. Hohwy, H.J. Jakobsen, M. Edén, M.H. Levitt, N.C. Nielsen, J. Chem. Phys. 108 (1998) 2686.
[29] C.G. Joo, A. Casey, C.J. Turner, R.G. Griffin, J. Am. Chem. Soc. 131 (2009) 12.
[30] X.L. Wang, Y.F. Yao, W.C. Qiao, J. Liang, W. Dong, K. Ma, J. Phys. Chem. C 125 (2021) 9908.
[31] V.S. Bajaj, M.L. Mak-Jurkauskas, M. Belenky, J. Herzfeld, R.G. Griffin, Proc. Natl. Acad. Sci. U. S. A. 106 (2009) 9244.
[32] Q.Z. Ni, T. Van Can, E. Daviso, M. Belenky, R.G. Griffin, J. Herzfeld, J. Am. Chem. Soc. 140 (2018) 4085.
[33] S. Xu, W. Zhang, X. Liu, X. Han, X. Bao, J. Am. Chem. Soc. 131 (2009) 13722.
[34] M. Hunger, M. Seiler, T. Horvath, Catal. Letters 57 (1999) 199.
[35] M. Hunger, T. Horvath, J. Weitkamp, Stud. Surf. Sci. Catal. 105 (B) (1997) 853.
[36] M. Hunger, T. Horvath, J. Chem. Soc. Chem. Commun. 1423 (1995).
[37] P. Berruyer, S. Björgvinsdóttir, A. Bertarello, G. Stevanato, Y. Rao, G. Karthikeyan, G. Casano, O. Ouari, M. Lelli, C. Reiter, F. Engelke, L. Emsley, J. Phys. Chem. Lett. 11 (2020) 8386.
[38] E. Barbet-Massin, A.J. Pell, J.S. Retel, L.B. Andreas, K. Jaudzems, W.T. Franks, A.J. Nieuwkoop, M. Hiller, V. Higman, P. Guerry, A. Bertarello, M.J. Knight, M. Felletti, T. Le Marchand, S. Kotelovica, I. Akopjana, K. Tars, M. Stoppini, V. Bellotti, M. Bolognesi, S. Ricagno, J.J. Chou, R.G. Griffin, H. Oschkinat, A. Lesage, L. Emsley, T. Herrmann, G. Pintacuda, J. Am. Chem. Soc. 136 (2014) 12489.
[39] J. Cui, J. Li, X. Peng, R. Fu, J. Magn. Reson. 284 (2017) 73.